**Dentomaxillofacial Radiology (2020) 50**, 20200068


birpublications.org/dmfr

RESEARCH ARTICLE

# MRI for the display of autologous onlay bone grafts during early healing—an experimental study

[1,2]Tabea Flügge, [3]Ute Ludwig, [3]Philipp Amrein, [2]Florian Kernen, [4]Kirstin Vach, [2]Johannes Maier and [2]Katja Nelson

*[1]Department of Oral and Maxillofacial Surgery, Charité – Universitätsmedizin Berlin, corporate member of Freie Universität Berlin, Humboldt-Universität zu Berlin, and Berlin Institute of Health, Berlin, Germany; [2]Department of Oral and Maxillofacial Surgery, Translational Implantology, Medical Center – University of Freiburg, Faculty of Medicine, University of Freiburg, Freiburg, Germany; [3]Department of Radiology, Medical Center – University of Freiburg, Faculty of Medicine, University of Freiburg, Freiburg, Germany; [4]Institute of Medical Biometry and Statistics, Faculty of Medicine and Medical Center - University of Freiburg, Freiburg, Germany*

**Objectives:** Autologous bone grafts are the gold standard to augment deficient alveolar bone. Dimensional graft alterations during healing are not known as they are not accessible to radiography. Therefore, MRI was used to display autologous onlay bone grafts in vivo during early healing.

**Methods and materials:** Ten patients with alveolar bone atrophy and autologous onlay grafts were included. MRI was performed with a clinical MR system and an intraoral coil preoperatively (t0), 1 week (t1), 6 weeks (t2) and 12 weeks (t3) postoperatively, respectively. The graft volumes were assessed in MRI by manual segmentation by three examiners. Graft volumes for each time point were calculated and dimensional alteration was documented. Cortical and cancellous proportions of bone grafts were assessed. The intraobserver and interobserver variability were calculated. Statistical analysis was performed using a mixed linear regression model.

**Results:** Autologous onlay bone grafts with cortical and cancellous properties were displayed *in vivo* in eight patients over 12 weeks. The fixation screws were visible as signal voids with a thin hyperintense fringe. The calculated volumes were between 0.12–0.74 $cm^3$ (t1), 0.15–0.73 $cm^3$ (t2), and 0.17–0.64 $cm^3$ (t3). Median changes of bone graft volumes of −15% were observed. There was no significant difference between the examiners ($p = 0.3$).

**Conclusions:** MRI is eligible for the display and longitudinal observation of autologous onlay bone grafts. Image artifacts caused measurements deviations in some cases and minimized the precise assessment of graft volume. To the knowledge of the authors, this is the first study that used MRI for the longitudinal observation of autologous onlay bone grafts.
*Dentomaxillofacial Radiology* (2020) **50**, 20200068. doi: 10.1259/dmfr.20200068

**Cite this article as:** Flügge T, Ludwig U, Amrein P, Kernen F, Vach K, Maier J, et al. MRI for the display of autologous onlay bone grafts during early healing—an experimental study. *Dentomaxillofac Radiol* 2020; **50**: 20200068.

**Keywords:** (MeSH): Magnetic Resonance Imaging; alveolar bone augmentation; dental implants; diagnostic imaging; artifacts

## Introduction

Despite the availability of a wide range of bone grafting techniques and materials that are used in clinical routine, the radiographic display of bone grafts has not been standardized and a multitude of variables leads to incongruent results for their display.[1–3] Nevertheless, imaging of bone grafts is crucial to assess the success of healing and integration of the graft and to select the

Correspondence to: Tabea Flügge, E-mail: tabea.fluegge@uniklinik-freiburg.de
Received 24 February 2020; revised 23 July 2020; accepted 05 August 2020

appropriate dimensions of a subsequently placed dental implant.

Radiographic examinations, especially tomographic imaging such as CT and cone-beam CT (CBCT), may display bone three-dimensionally, however limitations apply. Autologous onlay grafts imaged at an early healing time point are not adequately displayed due to their low degree of mineralization. Furthermore, bone block grafts are fixed to the underlying bone with titanium screws inducing artifacts in the form of streaks and extinctions and potentially mask the graft and surrounding structures.[4,5] The ionizing character of radiographic imaging and the accompanying health risks prohibit its repeated use and therefore exclude longitudinal studies.[6,7]

Dimensional changes of bone grafts may be estimated by the measurement of soft tissue alterations as demonstrated for dimensional changes of the alveolar crest after tooth extraction.[8] Measurement of soft tissue is easy to accomplish clinically or on individually fabricated stone cast.[9] The information, however, on three-dimensional dimensions of bone grafts is limited as the amount or thickness of the soft tissue is unknown. Furthermore, the bone quality during bone graft healing cannot be assessed with either technique.

The diagnostic capabilities of CT and CBCT in dental implantology are restricted to the display of mineralized tissues (bone, teeth) with a deficiency in the display of tissue with a low grade of mineralization (*e.g.,* bone transplants, hard tissue in regeneration/revascularization phase). CBCT has been used in studies evaluating synthetic or xenogenic bone replacement material with mineralized particles of high radio opacity.[10] Furthermore, dimensional changes of bone grafts were observed using CBCT, when high-density bone substitute materials or combinations of bone with bone substitute materials were used.[11–14]

CT has been used to display the dimensional changes of autologous bone grafts over time.[15–17] In CT, the density of tissues corresponds to Hounsfield units (HU), therefore applying a HU-based filter can give information on the tissue (*e.g.,* bone) quality and allow quantitative analysis of images. In CBCT, the displayed gray values vary and do not allow a standardized correlation with HU; therefore, the quantification and qualification of bone grafts using CBCT may not be accomplished.[6,18–20]

The lack of knowledge about the dimensions of bone grafts consequently due to the absence of an appropriate imaging method is addressed in this study.

MRI could be used as an alternative imaging modality for alveolar bone and bone grafts as it has proven successful to display the dento-alveolar complex using intraoral coils and standard MRI equipment for the head and neck region.[21–23] Furthermore, MRI may be used to display soft tissues and hard tissues with low mineralization. These two reasons predestine MRI for the display and longitudinal observation of autologous cortico-cancellous bone grafts.

MRI is increasingly used for imaging of the dento-maxillofacial complex. The indications for MRI include the delineation of the inferior alveolar nerve in healthy subjects and after iatrogenic injury; the detection of caries, pulpitis and periapical lesions; the localization of impacted teeth and dental implant planning.[24–30] High-resolution images, with voxel sizes of approximately 0.5 $mm^3$ and clinically feasible scanning times, are achieved with specific surface coils or intraoral coils.[22,23,31,32]

MRI has been used to display the maxillary sinus with incorporated bone substitute material and soft tissue swelling as well as blood retention after sinus augmentation procedures using autologous bone and various bone substitute materials.[33–38]

The use of MRI for the display of autologous onlay bone grafts fixed with titanium osteosynthesis screws has not been evaluated yet. A previously introduced intraoral coil was used for MRI to enhance image resolution and contrast.[22,23]

## Methods and materials

### *Patient selection*

In 10 patients, onlay bone grafting and MRI were performed. The study protocol was approved by the Institutional Review Board of the Medical Center – University of Freiburg, Freiburg, Germany (338/13). Written informed consent for the treatment was obtained from each participant. Patients were aged between 26 and 64 years (mean 52.5 years), three female and seven male patients were included. The bone graft region of each patient is displayed in Table 1.

### *Bone grafting*

The patients were partially edentulous and presented with an atrophic maxilla ($n$ = 6) or mandible ($n$ = 4). Out of 10 patients, eight patients received bone grafts from the iliac crest and two patients received bone grafts from the ascending ramus of the mandible. The surgical intervention was performed as previously described.[39]

**Table 1** Patient data and edentulous regions (FDI) that received bone grafts. *Patients had to be excluded for data analysis

| *patient* | *region of bone graft* | *donor region* | *age* | *gender* |
|---|---|---|---|---|
| 1 | 21 | iliac crest | 59 | female |
| 2 | 21 | iliac crest | 49 | female |
| 3* | 46 | retromolar | 59 | male |
| 4* | 31–32 | retromolar | 55 | male |
| 5 | 21–22 | iliac crest | 27 | male |
| 6 | 15–17 | iliac crest | 46 | male |
| 7 | 11 | iliac crest | 61 | male |
| 8 | 35–37 | iliac crest | 59 | female |
| 9 | 35–36 | iliac crest | 65 | male |
| 10 | 25–27 | iliac crest | 52 | male |

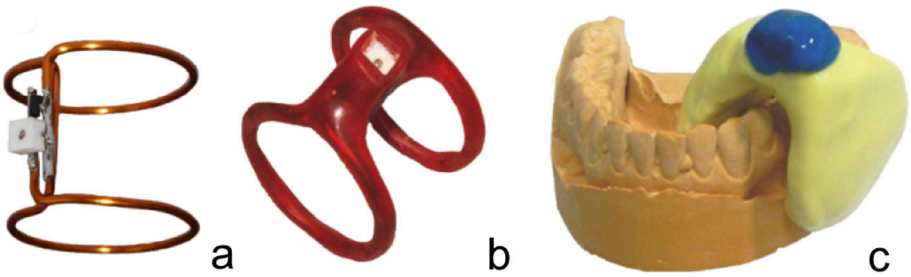


**Figure 1** Inductively coupled intraoral coil with variable capacitor and diodes before (a) and after resin coating (b), and adapted to the individual region of bone augmentation using a silicon coating (c). Figure adapted from previously published work.[23]

Iliac corticocancellous bone grafts were harvested from the medial cortical plate of the anterior superior rim by two horizontal and two vertical osteotomies with an oscillating saw and osteotomes. Bone grafts from the retromolar region of the mandible were harvested with a piezotome and osteotomes and consisted mostly of cortical bone. The bone grafts were adapted to the size of the edentulous alveolar ridges and fixed with the cancellous aspect facing the residual bone and the cortical aspects forming the labial and occlusal contour. Each bone graft was fixed with at least two osteosynthesis screws to avoid rotation. The grafted area was covered with a mobilized mucoperiostal flap after periosteal releasing incisions and closed with running and interrupted sutures.

*MR imaging*

MRI was performed preoperatively (t0), 1 week (t1), 6 weeks (t2) and 12 weeks (t3) postoperatively, respectively. A clinical whole-body MR system (Magnetom Prisma, Siemens Healthineers, Erlangen, Germany) equipped with a body transmit coil, a 4 cm receive loop coil (LC), and an intraoral inductively coupled coil (ICC) tuned to 123.195 MHz[2] for signal enhancement were used (Figure 1).[23] 2D Turbospinecho (TSE) sequences with 1 mm slice thickness and in plane resolution = 300×300 µm$^2$ were acquired. Depending on the desired image volume, the number of slices varied from 19 to 32, the matrix sizes were between 128×128 and 320×320 and the FOV was between 39×39 mm$^2$ and 111×111 mm$^2$. The acquisition time therefore varied between 2:38 and 5:03 min. Further image parameters were: TE/TR = 15/1860 ms, two averages, band width = 685 Hz/Px, number of echoes = 3, echo spacing between 7.32 and 7.9 ms. The view angle tilting (VAT) technique was applied to suppress image artifacts from susceptibility changes around titanium osteosynthesis screws.[40] VAT is a technique that is applied during MR image acquisition to compensate for possible distortions within each image plane. However, its application limits image resolution.[41]

*Data evaluation*

The following protocol was applied for data evaluation. Imaging data were collected and imported to Amira (V.6.5.0, Thermo Fisher Scientific, Waltham, MA, USA). The displayed range of signal intensity values was adjusted for each imaging sequence and not changed throughout evaluation to avoid bias. Each observer was calibrated using augmented and MRI imaged sheep jaws and introduced to the software to ensure common criteria for the identification of bone transplants and adjacent anatomical structures. The specimens were prepared in a preliminary animal study in which a bone graft harvested from the calvarium of a sheep was fixated with a titanium osteosynthesis screw to the edentulous part of its mandible. The gingival soft tissue was used to cover the bone graft in analogy to the clinical procedure. The specimens were imaged using the intraoral coil and identical MRI protocols. Each examiner received MR images of sheep jaws and after mutual inspection each examiner segmented the bone graft. Results of segmentation were again viewed by all three examiners. After evaluation of sheep specimens, the MR images of bone grafts in the study participants were evaluated.

The bone grafts and neighbouring structures were identified and located in the images. The vestibular and crestal outline of the bone graft consisted of cortical bone and was detected by its hypointense signal, directly adjacent to the hyperintense signal of the surrounding gingiva. In the vestibulo-oral direction, the cortical portion was followed by a hyperintense cancellous portion that was distinguished from the underlying residual bone with cortical properties. For evaluation, bone transplants were delineated in each slice of the imaging sequence. The total volume of each graft was obtained by adding the marked volume in each slice (Figure 2). Three examiners evaluated MR images of bone grafts taken at each interval and repeated measurements three times with a time-lag of two weeks between the measurements.

*Statistical analysis*

Intraobserver and interobserver variability for bone graft volumes were assessed as well as volume changes of bone grafts over time (t1–t3). Statistical analysis was performed using a mixed linear regression model (StataCorp. 2017. Stata Statistical Software: Release 15. College Station, TX: StataCorp LLC).

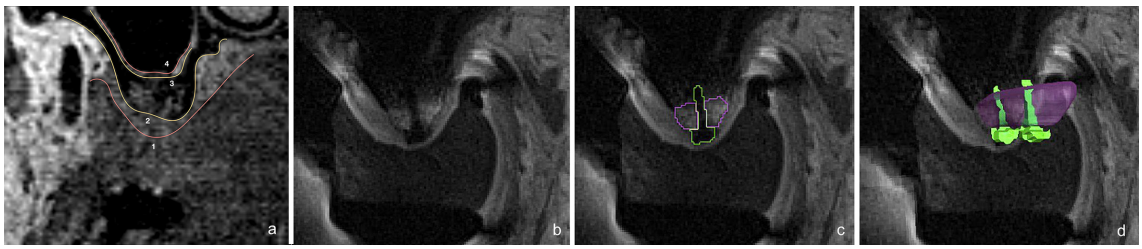


**Figure 2** Transversal cross-section through region 16 (FDI) preoperatively (t0) (a), with marked gingival outline (1), cortical bone outline (2), sinus floor (3) and Schneiderian membrane (4), postoperatively (t1) (b), with marked volume of bone graft (purple) and osteosynthesis screw (green) (c), and grafted bone volume by adding marked regions in every slice (d).

## Results

MRI of autologous onlay bone grafts was performed with intraoral coils *in vivo* in seven patients. Two patients with mandibular bone grafts were excluded within the course of the study due to claustrophobia during MR examination or due to non-precious-metal-reinforced provisional prostheses masking the augmented region.

In preoperative imaging, cortical bone areas were displayed with hypointense signal, whereas cancellous bone appeared with hyperintense signal. The gingival soft tissues surrounding cortical bone were displayed with hyperintense signal (Figure 3). Autologous bone grafts from the iliac crest ($n$ = 7) displayed cortical and cancellous properties that were visible with MRI at every stage (Figure 4). Further images show bone grafts in different regions of the jaw at different healing times (Figure 5).

The graft from the ascending ramus of the mandible was mostly cortical. The osteosynthesis screws used to fix the bone grafts were visible as signal voids surrounded by a thin hyperintense fringe.

The calculated volumes of the bone grafts were between 0.12–0.74 $cm^3$ at t1, 0.15–0.73 $cm^3$ at t2, and 0.17–0.64 $cm^3$ at t3. Median dimensional changes of bone graft volumes of −15% (Examiner 1),–17% (Examiner 2) and −9% (Examiner 3) were observed. The overall median dimensional changes of bone grafts were −15% (mean −5%). There was no significant difference between the examiners for overall dimensional changes of grafts ($p$ = 0.3). Numerical values are displayed in Table 2.

The standard deviation was 0.090 $mm^3$ (confidence interval0.051–0.158) for interexaminer variation and 0.061 (confidence interval 0.041–0.09) for intraexaminer variation.

## Discussion

Autologous bone grafts and their dimensional changes during healing were displayed with MRI. Median dimensional changes of −15% were observed over 12 weeks.

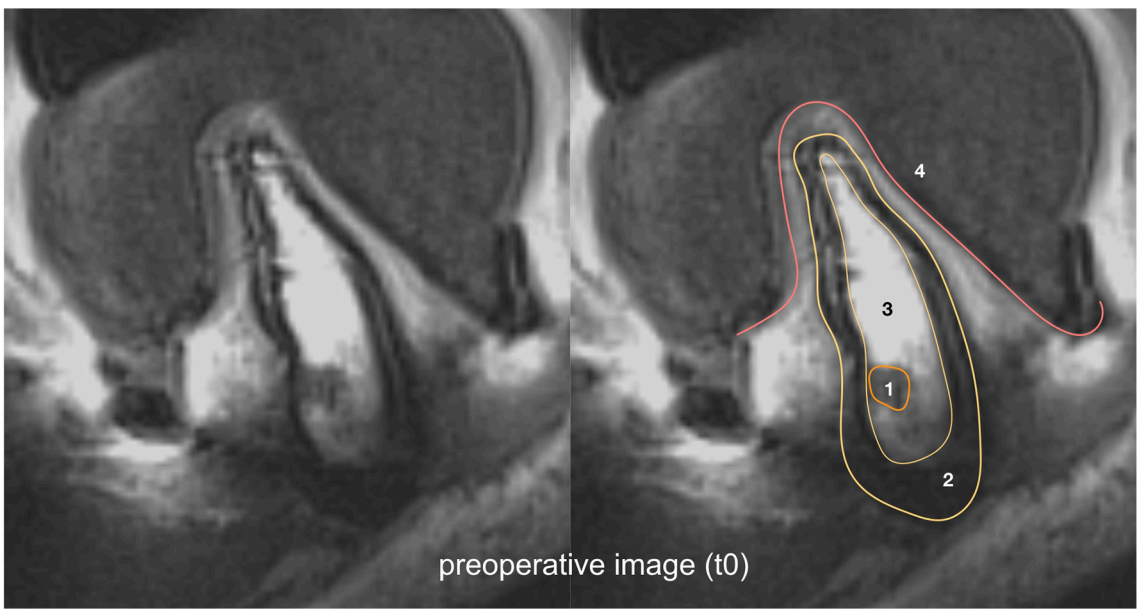


**Figure 3** Transversal cross-section in preoperative imaging of atrophic mandible (region 36-FDI) displaying the residual bone with inferior alveolar nerve (1), cortical bone (2), cancellous bone (3) and gingiva (4).

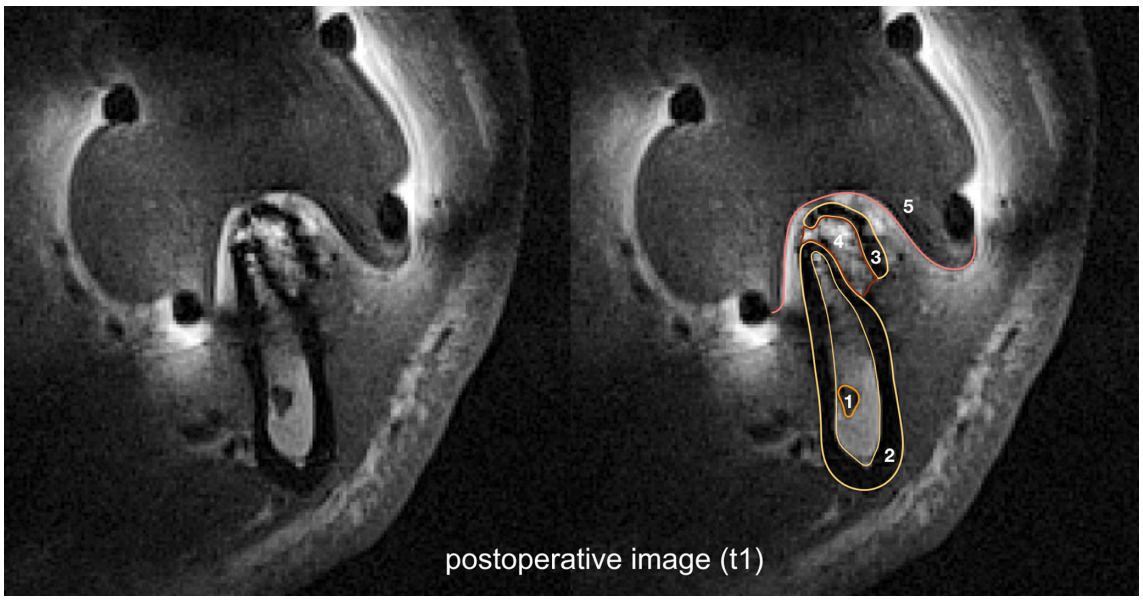


**Figure 4** Transversal cross-section through mandible in region 36 (FDI) displaying the residual bone with inferior alveolar nerve (1), cortical bone (2) and the bone transplant with cortical part (3) and cancellous part (4) covered by the mucoperiostal flap (5).

Previous studies on the dimensional changes of autologous bone grafts used repeated CT scans for volume assessment.[15–17] Barone et al documented iliac bone grafts with mean volumes of 0.94 $cm^3$ immediately after grafting and 0.69 $cm^3$ after a healing period of 4 months. The mean volume of bone grafts was generally higher, than in the presented study (0.43 $cm^3$ maxilla, 0.74 $cm^3$ mandible). Mean volume change of bone grafts was −29% and therefore also higher than in the presented study (−15%).[17] Sbordone et al examined dimensional changes of autologous iliac bone grafts between 3–5 and 12 months after augmentation surgery. Completely edentulous jaws or partially edentulous jaws, without further specifying the location, the number of missing teeth or the defect size, were treated. Mean bone graft volumes were 1.67 $cm^3$ and 1.96 $cm^3$ in the maxilla and mandible, respectively, and showed a dimensional change of −35% and −51%, respectively, between 3–5 and 12 months.[15] The dimensional changes of bone grafts within the first 3–5 months were not assessed radiographically. Bone graft volumes and dimensional changes were again significantly higher than in the presented study. In a comparable study, the volume of autologous iliac bone grafts was measured at 3–5 months (1.3 and 1.25 $cm^3$) and up to 6 years after augmentation surgery. The baseline volume of bone grafts (up to 3–5 months) however was not assessed radiographically and therefore the early healing could not be compared to the data in this study.[16] All three studies using CT for the measurement of dimensional changes of iliac bone grafts reported higher volumes of bone grafts and reported higher volume resorption. Lower resorption rates in the presented study may be caused by a favourable ratio of cortical and cancellous bone portions that was previously reported for a specific augmentation technique using bone grafts from the iliac crest.[42]

Previous studies have observed bone grafts with CT after a minimum healing period of 3 months.[15–17] CT and CBCT might be used to assess mineralized portions of transplanted bone. In contrast, MRI displays soft tissues and tissues with a low grade of mineralization.

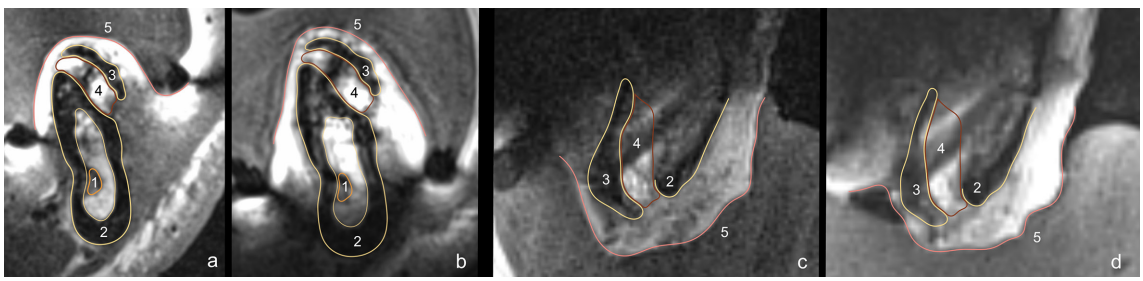


**Figure 5** Transversal cross-sections through mandible in region 46 (FDI) at t1 (a) and t2 (b) as well as transversal cross-sections through the maxilla in region 21 (FDI) at t2 (c) and t3 (d) displaying the residual bone with inferior with inferior alveolar nerve (1), cortical bone (2) and the bone transplant with cortical part (3) and cancellous part (4) covered by the mucoperiostal flap (5).

**Table 2** Median, mean (standard deviation – SD) for volume of bone grafts (in $cm^3$) at each time point in each patient. Marked volumes are displayed in Figure 5a–d.

| *patient* | *t1* | | *t2* | | *t3* | |
|---|---|---|---|---|---|---|
| | **mean (SD)** | **median** | **mean (SD)** | **median** | **mean (SD)** | **median** |
| **1** | 0.12 (0.03) | 0.13 | 0.154 (0.03) | 0.16 | 0.16 (0.03) | 0.15 |
| **2** | 0.22 (0.05) | 0.21 | 0.173 (0.08)[5c] | 0.13 | 0.19 (0.03)[5d] | 0.18 |
| **4** | - | | 0.407 (0.23) | 0.37 | 0.30 (0.08) | 0.29 |
| **6** | 0.72 (0.06) | 0.72 | - | | 0.65 (0.07) | 0.63 |
| **7** | 0.20 (0.05) | 0.21 | 0.187 (0.03) | 0.18 | 0.17 (0.03) | 0.16 |
| **8** | 0.79 (0.16) | 0.75 | 0.711 (0.08) | 0.71 | 0.64 (0.08) | 0.65 |
| **9** | 0.70 (0.11)[5a] | 0.66 | 0.596 (0.09)[5b] | 0.60 | - | |
| **10** | 0.87 (0.27) | 0.80 | - | | - | |

MRI might be favourable for the assessment of early bone healing, during which the mineralization of grafts has not taken place.

This is the first study to use MRI for the display of autologous onlay grafts and to measure the dimensional changes of bone grafts *in vivo* over time. In previous MRI studies, measurement of grafted volumes was not performed.[36,38] Only in one postoperative MR scan the augmented area was measured favourable changes over time were not evaluated.[33,35,37] One case report noted stable vertical bone dimensions between 10 days and 10 weeks after maxillary sinus augmentation with particulate iliac bone in one patient.[34]

Most previous studies administered contrasting agent intravenously prior to MR imaging.[33–35,38] The administration of contrasting agent was not necessary in this study, as T2W imaging protocols were used with the intraoral coil and enabled high contrast in the field of view.

MRI acquisition times varied between 5:16 min and 10:00 min in existing studies and were therefore longer than the acquisition time of 2:38 min in this study.[33,34,37,38] Short acquisition times are intended *in vivo*, to minimize discomfort of the patient and artifacts due to patient movement.

An intraoral coil was used to enhance contrast and improve image resolution in the region of interest.[22,23] An unprecedented in-plane image resolution of 300×300 µm and 1 mm slice thickness were achieved which is comparable to CBCT. This is accomplished with an intraoral coil and a small image volume. With the use of standard head and neck coils, a surface coil for dental imaging or smaller surface coils that were adapted to the respective side of the face, the image resolution of MRI is limited to around 0.5 $mm^3$.[24,30,43,44] Previous studies of bone augmentation using MRI applied standard MRI equipment and achieved image resolutions over 700×700 µm with slice thicknesses up to 4 mm.[33,34,37]

The bone grafts could be delineated in cortical (hypointense) and cancellous (hyperintense) parts. The surrounding mucosa was displayed with hyperintense signal. One previous study characterized bone as hypointense and bovine bone mineral material in the maxillary sinus was initially as hyperintense and not clearly distinguished from swollen mucosa in T1W MR images. Bone regeneration was interpreted, when the augmentation material appeared hypointense in T1 images after 104 days.[38] Other studies did not describe appearance of bone grafts in MR images and described mucosal swelling, exudate or blood retention in the maxillary sinus, all presenting with hyperintense signal in MR images.[34,36]

The delineation of bone grafts was performed by three examiners at the three different time points. The results for intraexaminer variation showed a wide confidence interval, which was interpreted as the difficulty to repeatably identify the bone graft outlines, especially in the presence of artifacts originating from osteosynthesis screws, dental restorations of adjacent teeth and in one patient a neighbouring dental implant. Previous studies onbone graft dimensions did not include repeated measurements of bone grafts and multiple examiners, respectively.[15–17] Therefore, no comparison can be made. To date there is a lack of an *in vivo* imaging method and evaluation protocol, which can be considered a validated and reliable standard to quantify the volume of bone grafts.

In one participant (no.1), an increase of bone volume between t1 and t3 was observed. This effect was explained with an imprecise measurement of graft volume due to image artifacts originating from surrounding teeth with metallic restorations. A high standard deviation and deviation between mean and median bone volumes underlines the difficulty to clearly delineate the graft volume in MR images of some participants.

Artifacts originating from titanium osteosynthesis screws were found in preliminary imaging of bone grafts in sheep jaws and were regarded as hindrance to display autologous onlay grafts with MRI (unpublished data). Using the VAT technique, these artifacts could be minimized, and bone grafts could be displayed with MRI. The benefit of artefact suppression with the VAT technique is associated with the compromise of a lower image resolution. It resulted in non-isometric image resolution which is a limitation with regard to multi planar display for subsequent implant planning. However, it did not hinder adequate measurement of bone grafts and was therefore beneficial in this study.

One limitation of this study was that the intraoral coil could not be placed due to postoperative mucosal swelling and mobilization of mucosa and subsequent flattening of the vestibulum. Especially in the first postoperative MR scan (1 week postoperatively), this led to a lower signal in the augmented region. The development of MR protocols producing comparable image quality not using an intraoral coil, but a standard head coil, could help to overcome that limitation, inherent to bone augmentation sites.

MRI is a safe procedure, if contraindications such as cardiac pacemakers, mechanical heart valves, metallic surgical clips and metallic foreign bodies are carefully regarded.[45] Claustrophobia and vast dental restorations are as well contraindications to MR imaging and were the reason for drop-out of three participants in this study.

## Conclusion

To the knowledge of the authors, this is the first study that used MRI for the longitudinal observation of early healing of autologous onlay bone grafts. MRI is eligible for the display of autologous onlay bone grafts and longitudinal observation of bone graft dimension. In spite of the high image resolution achieved when using intraoral coils, artifacts and postoperative swelling complicate the reproducible delineation of grafts in the early healing period.

## Funding

The project (14-157) was supported by a grant from the Osteology Foundation, Switzerland.

## REFERENCES

1. Fretwurst T, Gad LM, Nelson K, Schmelzeisen R. Dentoalveolar reconstruction: modern approaches. *Curr Opin Otolaryngol Head Neck Surg* 2015; **23**: 316–22. doi: https://doi.org/10.1097/MOO.0000000000000167
2. Buser D, Dula K, Hess D, Hirt HP, Belser UC. Localized ridge augmentation with autografts and barrier membranes. *Periodontol 2000* 1999; **19**: 151–63. doi: https://doi.org/10.1111/j.1600-0757.1999.tb00153.x
3. Spin-Neto R, Marcantonio E, Gotfredsen E, Wenzel A. Exploring CBCT-based DICOM files. A systematic review on the properties of images used to evaluate maxillofacial bone grafts. *J Digit Imaging* 2011; **24**: 959–66. doi: https://doi.org/10.1007/s10278-011-9377-y
4. Schulze RKW, Berndt D, d'Hoedt B. On cone-beam computed tomography artifacts induced by titanium implants. *Clin Oral Implants Res* 2010; **21**: 100–7. doi: https://doi.org/10.1111/j.1600-0501.2009.01817.x
5. Schulze R, Heil U, Gross D, Bruellmann DD, Dranischnikow E, Schwanecke U, et al. Artefacts in CBCT: a review. *Dentomaxillofac Radiol* 2011; **40**: 265–73. doi: https://doi.org/10.1259/dmfr/30642039
6. Jacobs R, Salmon B, Codari M, Hassan B, Bornstein MM. Cone beam computed tomography in implant dentistry: recommendations for clinical use. *BMC Oral Health* 2018; **18**: 88. doi: https://doi.org/10.1186/s12903-018-0523-5
7. Wu T-H, Lin W-C, Chen W-K, Chang Y-C, Hwang J-J. Predicting cancer risks from dental computed tomography. *J Dent Res* 2015; **94**: 27–35. doi: https://doi.org/10.1177/0022034514554226
8. Tan WL, Wong TLT, Wong MCM, Lang NP. A systematic review of post-extractional alveolar hard and soft tissue dimensional changes in humans. *Clin Oral Implants Res* 2012; **23**(Suppl 5): 1–21. doi: https://doi.org/10.1111/j.1600-0501.2011.02375.x
9. Flügge T, Nelson K, Nack C, Stricker A, Nahles S. 2-Dimensional changes of the soft tissue profile of augmented and non-augmented human extraction sockets: a randomized pilot study. *J Clin Periodontol*(eds 2015; **42**: 390–7. doi: https://doi.org/10.1111/jcpe.12386
10. Domingues EP, Ribeiro RF, Horta MCR, Manzi FR, Côsso MG, Zenóbio EG. Vertical augmentation of the posterior atrophic mandible by interpositional grafts in a split-mouth design: a human tomography evaluation pilot study. *Clin Oral Implants Res* 2017; **28**: e193–200. doi: https://doi.org/10.1111/clr.12985
11. Buser D, Chappuis V, Bornstein MM, Wittneben J-G, Frei M, Belser UC. Long-Term stability of contour augmentation with early implant placement following single tooth extraction in the esthetic zone a prospective, cross-sectional study in 41 patients with a 5- to 9-year follow-up. *J Periodontol* 2013; **19**: 1–16. doi: https://doi.org/10.1902/jop.2013.120635
12. Kuchler U, Chappuis V, Gruber R, Lang NP, Salvi GE. Immediate implant placement with simultaneous guided bone regeneration in the esthetic zone: 10-year clinical and radiographic outcomes. *Clin Oral Implants Res*(eds 2016; **27**: 253–7. doi: https://doi.org/10.1111/clr.12586
13. Chappuis V, Rahman L, Buser R, Janner SFM, Belser UC, Buser D. Effectiveness of contour augmentation with guided bone regeneration: 10-year results. *J Dent Res*(eds 2018; **97**: 266–74. doi: https://doi.org/10.1177/0022034517737755
14. Chappuis V, Cavusoglu Y, Buser D, von Arx T. Lateral ridge augmentation using autogenous block grafts and guided bone regeneration: a 10-year prospective case series study. *Clin Implant Dent Relat Res* 2017; **19**: 85–96. doi: https://doi.org/10.1111/cid.12438
15. Sbordone L, Toti P, Menchini-Fabris GB, Sbordone C, Piombino P, Guidetti F. Volume changes of autogenous bone grafts after alveolar ridge augmentation of atrophic maxillae and mandibles. *Int J Oral Maxillofac Surg* 2009; **38**: 1059–65. doi: https://doi.org/10.1016/j.ijom.2009.06.024
16. Sbordone C, Toti P, Guidetti F, Califano L, Santoro A, Sbordone L. Volume changes of iliac crest autogenous bone grafts after vertical and horizontal alveolar ridge augmentation of atrophic maxillas and mandibles: a 6-year computerized tomographic follow-up. *Journal of Oral and Maxillofacial Surgery* 2012; **70**: 2559–65. doi: https://doi.org/10.1016/j.joms.2012.07.040
17. Barone A, Toti P, Menchini-Fabris G-B, Felice P, Marchionni S, Covani U. Early volumetric changes after vertical augmentation of the atrophic posterior mandible with interpositional block graft versus onlay bone graft: a retrospective radiological study. *J Craniomaxillofac Surg* 2017; **45**: 1438–47. doi: https://doi.org/10.1016/j.jcms.2017.01.018
18. Mah P, Reeves TE, McDavid WD. Deriving Hounsfield units using grey levels in cone beam computed tomography. *Dentomaxillofac Radiol* 2010; **39**: 323–35. doi: https://doi.org/10.1259/dmfr/19603304
19. Pauwels R, Jacobs R, Singer SR, Mupparapu M. CBCT-based bone quality assessment: are Hounsfield units applicable? *Dentomaxillofac Radiol* 2015; **44**: 20140238. doi: https://doi.org/10.1259/dmfr.20140238
20. Scarfe WC, Li Z, Aboelmaaty W, Scott SA, Farman AG. Maxillofacial cone beam computed tomography: essence, elements and

steps to interpretation. *Aust Dent J* 2012; **57 Suppl 1**(1 Suppl): 46–60. doi: https://doi.org/10.1111/j.1834-7819.2011.01657.x

21. Hövener J-B, Zwick S, Leupold J, Eisenbeiß A-K, Scheifele C, Schellenberger F, et al. Dental MRI: imaging of soft and solid components without ionizing radiation. *J Magn Reson Imaging* 2012; **36**: 841–6. doi: https://doi.org/10.1002/jmri.23712
22. Flügge T, Hövener J-B, Ludwig U, Eisenbeiss A-K, Spittau B, Hennig J, et al. Magnetic resonance imaging of intraoral hard and soft tissues using an intraoral coil and flash sequences. *Eur Radiol* 2016; **26**: 4616–23. doi: https://doi.org/10.1007/s00330-016-4254-1
23. Ludwig U, Eisenbeiss A-K, Scheifele C, Nelson K, Bock M, Hennig J, et al. Dental MRI using wireless intraoral coils. *Sci Rep* 2016; **6**: 1. doi: https://doi.org/10.1038/srep23301
24. Kreutner J, Hopfgartner A, Weber D, Boldt J, Rottner K, Richter E, et al. High isotropic resolution magnetic resonance imaging of the mandibular canal at 1.5 T: a comparison of gradient and spin echo sequences. *Dentomaxillofac Radiol* 2017; **46**: 20160268. doi: https://doi.org/10.1259/dmfr.20160268
25. Wanner L, Ludwig U, Hövener J-B, Nelson K, Flügge T. Magnetic resonance imaging-a diagnostic tool for postoperative evaluation of dental implants: a case report. *Oral Surg Oral Med Oral Pathol Oral Radiol* 2018; **125**: e103–7. doi: https://doi.org/10.1016/j.oooo.2018.01.005
26. Bracher A-K, Hofmann C, Bornstedt A, Hell E, Janke F, Ulrici J, et al. Ultrashort echo time (Ute) MRI for the assessment of caries lesions. *Dentomaxillofac Radiol* 2013; **42**: 20120321. doi: https://doi.org/10.1259/dmfr.20120321
27. Cankar K, Vidmar J, Nemeth L, Serša I. T2 mapping as a tool for assessment of dental pulp response to caries progression: an in vivo MRI study. *Caries Res* 2020; **54**: 23–34.
28. Juerchott A, Pfefferle T, Flechtenmacher C, Mente J, Bendszus M, Heiland S, et al. Differentiation of periapical granulomas and cysts by using dental MRI: a pilot study. *Int J Oral Sci* 2018; **10**: 1–8. doi: https://doi.org/10.1038/s41368-018-0017-y
29. Kirnbauer B, Jakse N, Rugani P, Schwaiger M, Magyar M. Assessment of impacted and partially impacted lower third molars with panoramic radiography compared to MRI-a proof of principle study. *Dentomaxillofac Radiol* 2018; **47**: 20170371. doi: https://doi.org/10.1259/dmfr.20170371
30. Flügge T, Ludwig U, Hövener J-B, Kohal R, Wismeijer D, Nelson K. Virtual implant planning and fully guided implant surgery using magnetic resonance imaging-Proof of principle. *Clin Oral Implants Res* 2020; **31**: 575–83. doi: https://doi.org/10.1111/clr.13592
31. Gradl J, Höreth M, Pfefferle T, Prager M, Hilgenfeld T, Gareis D, et al. Application of a dedicated surface coil in dental MRI provides superior image quality in comparison with a standard coil. *Clin Neuroradiol* 2017; **27**: 371–8. doi: https://doi.org/10.1007/s00062-016-0500-9
32. Idiyatullin D, Corum C, Moeller S, Prasad HS, Garwood M, Nixdorf DR. Dental magnetic resonance imaging: making the invisible visible. *J Endod* 2011; **37**: 745–52. doi: https://doi.org/10.1016/j.joen.2011.02.022
33. Gray CF, Redpath TW, Smith FW, Staff RT, Bainton R. Assessment of the sinus lift operation by magnetic resonance imaging. *Br J Oral Maxillofac Surg* 1999; **37**: 285–9. doi: https://doi.org/10.1054/bjom.1999.0073
34. Gray CF, Staff RT, Redpath TW, Needham G, Renny NM. Assessment of maxillary sinus volume for the sinus lift operation by three-dimensional magnetic resonance imaging. *Dentomaxillofac Radiol* 2000; **29**: 154–8. doi: https://doi.org/10.1038/sj.dmfr.4600518
35. Gray CF, Redpath TW, Bainton R, Smith FW. Magnetic resonance imaging assessment of a sinus lift operation using reoxidised cellulose (Surgicel) as graft material. *Clin Oral Implants Res* 2001; **12**: 526–30. doi: https://doi.org/10.1034/j.1600-0501.2001.120514.x
36. Wilkert-Walter C, Jänicke S, Spüntrup E, Th L. Examination of the maxillary sinus after sinus floor augmentation combined with autologous onlay osteoplasty. *Mund-, Kiefer- und Gesichtschirurg* 2002; **6**: 336–40.
37. Senel FC, Duran S, Icten O, Izbudak I, Cizmeci F. Assessment of the sinus lift operation by magnetic resonance imaging. *Br J Oral Maxillofac Surg* 2006; **44**: 511–4. doi: https://doi.org/10.1016/j.bjoms.2006.02.004
38. Sauerbier S, Palmowski M, Vogeler M, Nagursky H, Al-Ahmad A, Fisch D, et al. Onset and maintenance of angiogenesis in biomaterials: in vivo assessment by dynamic contrast-enhanced MRI. *Tissue Eng Part C Methods* 2009; **15**: 455–62. doi: https://doi.org/10.1089/ten.tec.2008.0626
39. Fretwurst T, Wanner L, Nahles S, Raguse JD, Stricker A, Metzger MC, et al. A prospective study of factors influencing morbidity after iliac crest harvesting for oral onlay grafting. *J Craniomaxillofac Surg* 2015; **43**: 705–9. doi: https://doi.org/10.1016/j.jcms.2015.03.023
40. Cho ZH, Kim DJ, Kim YK. Total inhomogeneity correction including chemical shifts and susceptibility by view angle tilting. *Med Phys* 1988; **15**: 7–11. doi: https://doi.org/10.1118/1.596162
41. Hargreaves BA, Worters PW, Pauly KB, Pauly JM, Koch KM, Gold GE. Metal-Induced artifacts in MRI. *AJR Am J Roentgenol* 2011; **197**: 547–55. doi: https://doi.org/10.2214/AJR.11.7364
42. Fretwurst T, Nack C, Al-Ghrairi M, Raguse JD, Stricker A, Schmelzeisen R, et al. Long-Term retrospective evaluation of the peri-implant bone level in onlay grafted patients with iliac bone from the anterior superior iliac crest. *J Craniomaxillofac Surg* 2015; **43**: 956–60. doi: https://doi.org/10.1016/j.jcms.2015.03.037
43. Juerchott A, Freudlsperger C, Weber D, Jende JME, Saleem MA, Zingler S, et al. In vivo comparison of MRI- and CBCT-based 3D cephalometric analysis: beginning of a non-ionizing diagnostic era in craniomaxillofacial imaging? *Eur Radiol* 2020; **30**: 1488–97. doi: https://doi.org/10.1007/s00330-019-06540-x
44. Juerchott A, Freudlsperger C, Zingler S, Saleem MA, Jende JME, Lux CJ, et al. In vivo reliability of 3D cephalometric landmark determination on magnetic resonance imaging: a feasibility study. *Clin Oral Investig* 2020; **24**: 1339–49. doi: https://doi.org/10.1007/s00784-019-03015-7
45. Dill T. Contraindications to magnetic resonance imaging: non-invasive imaging. *Heart* 2008; **94**: 943–8. doi: https://doi.org/10.1136/hrt.2007.125039